3D multiscale inversion of airborne electromagnetic data

Yang Su[1], Changchun Yin[1*], Libao Wang[2], Yunhe Liu[1], Bo Zhang[1], Xiuyan Ren[1], and Jun Li[1]
[1]College of Geoexploration Science and Technology, Jilin University, Changchun, China.
[2]Shandong Huichuang Technology Co., Ltd
yinchangchun@jlu.edu.cn

SUMMARY

Airborne electromagnetic (AEM) technology is an efficient geophysical exploration tool for investigating subsurface resistivity structures. To alleviate the problems with the resolution and computational efficiency for three-dimensional (3D) AEM inversion, we establish a relationship between coarse and fine grids in the inversion process based on shearlet transform, and propose a 3D multi-scale (MS) shearlet-based regularization inversion algorithm. The shearlet-based regularization inversion can effectively recover the anisotropic structure of anomalous bodies such as curved boundaries, and thus can significantly improve the resolution of the inversion results. In the initial stage of inversion, the coarse grid and sparse data points are used to recover the main structure of the subsurface. After the inversion reaches a certain level, the result from the coarse-grid inversion is used as coarse-scale model for shearlet structures in fine grids. After that, we continue to use fine grids and dense data points for our inversion, so that we can finally obtain the high-resolution inversions on the fine grids. This inversion method from coarse to fine grids can effectively reduce calculation time while ensuring high-resolution of inversions. We demonstrate the effectiveness and practicality of 3D MS inversion algorithm by using a synthetic example. The numerical experiments show that our MS method can effectively reduce the computational time without reducing resolution in AEM inversions.

Keywords: 3D inversion, airborne electromagnetic (AEM), multi-scale (MS) inversion, shearlet transform.

INTRODUCTION

Airborne electromagnetic (AEM) exploration method is frequently applied in fields such as mineral exploration, geothermal and groundwater detection, geological hazard prediction, environmental and engineering investigation due to its advantages of low cost and high efficiency. At present, the inversion method of AEM data are mainly based on the Tikhonov regularized inversion algorithm of gradient type that can reduce the non-uniqueness of the inversion and make the inversion relatively stable. The inversion algorithm of gradient type mainly includes conjugate gradient (CG), nonlinear conjugate gradient (NLCG), quasi Newton and Gauss Newton (GN) algorithm (Egbert et al., 2012; Long et al., 2020).

In recent years, scholars have introduced sparse transform into regularized inversions. Since the shearlet transform is a multiscale (MS) and multi-directional sparse transform, the model structures at different scales can be obtained by performing shearlet transformation to the original resistivity model. The coarsest-scale model reveals the integrated view, while the fine-scale model reveals the detailed edge structures of the target objects (Kutyniok et al., 2011). One can first restore the sparse coefficients at different shearlet scales in the iterative inversion process, and then restore the high-resolution structures of the model in the spatial domain.

In airborne EM we need to calculate EM responses for multiple transmitting sources in the iterative inversion process, which will inevitably generate huge amount of computations. Moreover, we know that gradient-type inversions invert the coarse structure first and then characterize the fine structures of the model. Therefore, we propose an inversion process from coarse to fine grids. We first use coarse grids and sparse survey data for our inversion at the initial stage until we obtain an overview of the model. Then, we take the results from the coarse-grid inversions as the coarsest scale model in the shearlet multi-scale structure, and use more refined mesh and dense survey data for our subsequent inversions. From the sparse coefficients restored at fine scales, we can improve the resolution of the boundary structures. This coarse-to-fine inversion strategy can ensure the resolution of the inversion results and reduce the computational time of 3D AEM inversions.

METHODS

The objective function for the shearlet-based inversion can be defined as (Su, et al., 2022)

$$\Phi = \varphi_d^n(\boldsymbol{p}) + \lambda^n \varphi_s^n(\boldsymbol{q}), \quad (1)$$

where φ_d and φ_s are the data misfit and shearlet coefficient regularization term, respectively. λ is the trade-off parameter that balances the relative contributions of these terms. $\boldsymbol{p}$ and $\boldsymbol{q}$ can be written in the following format, i.e.

$$\boldsymbol{p} = \mathbf{W}_d(\boldsymbol{d}^{obs} - \boldsymbol{d}^{n-1} - \mathbf{J}\delta\boldsymbol{m}), \tag{2}$$

$$\boldsymbol{q} = \mathbf{W}_s(\boldsymbol{m}^{n-1} + \delta\boldsymbol{m} - \boldsymbol{m}^{ref}), \tag{3}$$

where $\mathbf{W}_d$ is the reciprocals of the estimates to the standard deviations of the data noise. $\boldsymbol{d}^{obs}$ denotes the observed data, $\boldsymbol{d}^{n-1}$ denotes the responses calculated from the model $\boldsymbol{m}^{n-1}$, $\delta\boldsymbol{m}$ denotes the model updates of the nth iteration, $\boldsymbol{m}^{ref}$ denotes the reference model. Furthermore, we can obtain the derivative of the data fitting term with respect to the coefficient update, i.e.

$$\frac{\partial \varphi_d^n(\boldsymbol{p})}{\partial \delta\tilde{\boldsymbol{m}}} = (-\mathbf{W}_d\mathbf{J}\mathbf{W}_s^{-1})^T\mathbf{R}_d\mathbf{W}_d(\boldsymbol{d}^{obs} - \boldsymbol{d}^{n-1} - \mathbf{J}\delta\boldsymbol{m}), \tag{4}$$

where $\mathbf{W}_s^{-1}$ represents the inverse sparse transform operator. For the sparse regularization term, the derivative with respect to the coefficient updates can be written as

$$\frac{\partial \varphi_s^n(\boldsymbol{q})}{\partial \delta\tilde{\boldsymbol{m}}} = \mathbf{R}_s\mathbf{W}_s(\boldsymbol{m}^{n-1} + \delta\boldsymbol{m} - \boldsymbol{m}^{ref}) = \mathbf{R}_s\delta\tilde{\boldsymbol{m}} - \mathbf{R}_s(\tilde{\boldsymbol{m}}^{ref} - \tilde{\boldsymbol{m}}^{n-1}). \tag{5}$$

Here, we use the GN method to iteratively minimize the objective function. Then, minimizing (1) and combining (4) and (5), we obtain the linear equations system for our sparsely regularized inversion in the n^{th} inversion iteration, i.e.

$$(\mathbf{W}_s\mathbf{J}^T\mathbf{W}_d^T\mathbf{R}_d\mathbf{W}_d\mathbf{J}\mathbf{W}_s^{-1} + \lambda^n\mathbf{R}_s)\delta\tilde{\boldsymbol{m}} = \mathbf{W}_s\mathbf{J}^T\mathbf{W}_d^T\mathbf{R}_d\mathbf{W}_d(\boldsymbol{d}^{obs} - \boldsymbol{d}^{n-1}) + \lambda^n\mathbf{R}_s(\tilde{\boldsymbol{m}}^{ref} - \tilde{\boldsymbol{m}}^{n-1}). \tag{6}$$

We introduce the IRLS method to convert the inversion problem based on L1-norm regularization into a classic linear least-squares one in the above equation. For each iteration, the CG method is used to solve the linear equations (6) to get the sparse coefficients update $\delta\tilde{\boldsymbol{m}}$, then the model update in the spatial domain can be expressed as

$$\boldsymbol{m}^n = \boldsymbol{m}^{n-1} + s\mathbf{W}_s^{-1}\delta\tilde{\boldsymbol{m}}^n, \tag{7}$$

where s is the scale factor determined by a linear search.

The gradient-based regularized inversions gradually recover the model structures from coarse to fine scales. This inspires us to use coarse grids and sparse data for our inversions at the initial stage until an integral view of the model is obtained (as shown in Figure 1a and 1b). Then, we set the inversion results as the coarsest-scale model in the multiscale shearlet structure, and a more refined mesh and dense survey data are used for subsequent inversions (Figure 1c). In the subsequent inversions, the sparse coefficients at the fine scales can be further restored, which can improve the resolution of the boundary structures in the final inversion model (Figure 1d). The inversion process of dividing the grids from coarse to fine scales can reduce the computational time in 3D inversions and thus improve the efficiency in AEM data interpretations.

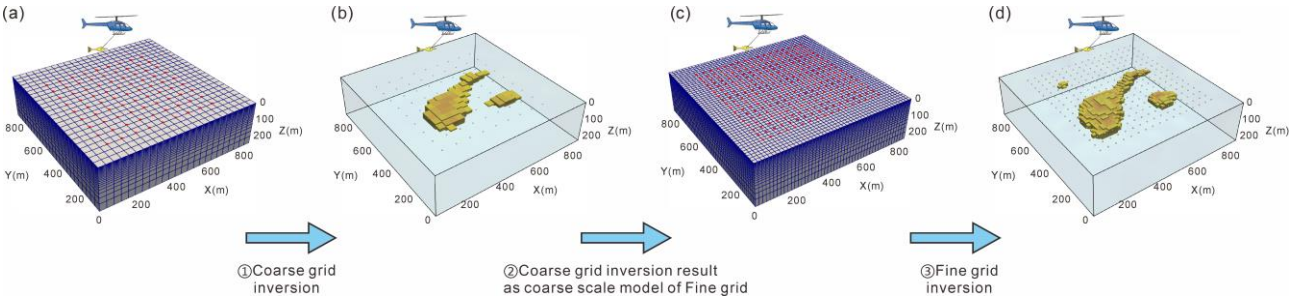

Figure 1. Schematic diagram of multi-scale inversions. (a) Initial coarse grids and sparse survey data; (b) coarse grids inversion results; (c) fine grids and dense survey data; (d) fine grids inversion result.

RESULTS

We take the frequency-domain Helicopter EM system (HEM) from Norway Geological Survey (NGU) as example. The system has three horizontal coplanar (HCP) coils and two vertical coaxial (VCX) coil pairs. The coarse-grid model we designed is a regular hexahedron with 32 cells. The width of each grid is 30 m, extending 960 m long in the x- and y-directions, respectively. In the z-direction, the total depth is about 320 m. There is a total of 9 survey lines, each of which has 9 survey points. The spacing of survey lines and points are both 80 m. A total of 81 survey stations are evenly distributed within the central area. The fine-grid model we designed has 64 cells and the width of each grid is

15 m, extending 960 m in the *x*- and *y*-direction, respectively. The subdivision of fine grids in the *z*-direction is consistent with that of coarse grids. There is a total of 17 survey lines, each of which has 17 survey points for dense grids. The spacings of the survey line and points are both 45 m. A total of 289 survey points are evenly distributed within the central area of the synthetic model. Moreover, we assume 9 evenly-distributed blocks with high (1000 Ω·m) and low (10 Ω·m) resistivities within a half-space of 100 Ω·m (Figure 2a). The initial model for our inversion is a half-space of 100 Ω·m. The initial regularization factor is assumed to be 10. For shearlet-based inversions, we set the shearlet system that contains 1 coarse scale and 3 fine scales. We add 5% Gaussian noise to the synthetic data.

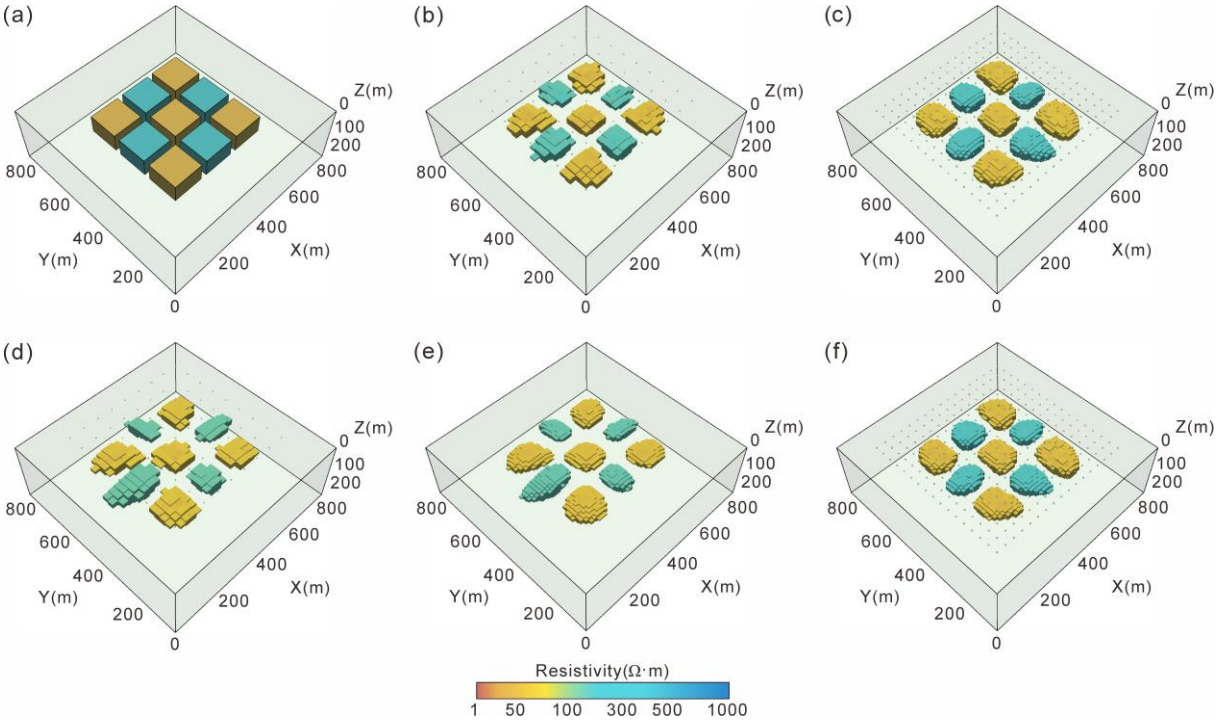

Figure 2. Comparison of inversion results for Model 1. (a) The true model; (b) inversion results of coarse grids with sparse survey data; (c) inversion results of fine grids with dense survey points; (d) inversion results of sparse survey data on coarse grids when the RMSs decrease to 1.3; (e) space-domain model of fine grids obtained by using the results of (d) as coarse-scale coefficients in the shearlet system, and then setting the fine scale coefficients to 0 and performing inverse shearlet transform; (f) multiscale inversion results.

Figures 2b shows the inversion results of coarse grids with sparse survey points, while Figures 2c shows the results of fine grids with dense survey points. It is seen that the resolution of fine grids with dense survey points are very high. The inversion results of the fine grids provide more details on boundary information of the synthetic model. Figures 2d-2f show the results of shearlet-based coarse-to-fine-grids inversion results. Figures 2d shows the inversion results for the coarse grids with sparse survey points after the RMS reduces to 1.3, while Figures 2f shows the results of the fine grids in spatial domain obtained by taking the results of Figures 2e as the coarse-scale coefficients in the shearlet system, and then setting the fine-scale coefficients to 0 and performing inverse shearlet transform. Figures 2f shows the final inversion results from the fine-scale grids with dense survey points. It is seen that the resolution of the inversion results is similar to that of the fine-scale grids with dense survey points in Figures 2c. This verifies again that our multiscale inversions can obtain the same resolution as the fine-grid inversion. Table 1 and Figure 3 give the inversion parameters versus iterations and the time consumption. It is seen that although the three inversion schemes converge stably, our coarse-to-fine-grids inversions save 41% of calculation time.

Table 1. Parameters for our MS inversions

	Coarse grid	Fine grid	MS (coarse grid)	MS (fine grid)
Iteration	14	17	1-11	12-19
Data misfit (rms)	1.023	1.052	1.255	1.042
Calculation time (h)	1.63	6.92	0.92	3.18

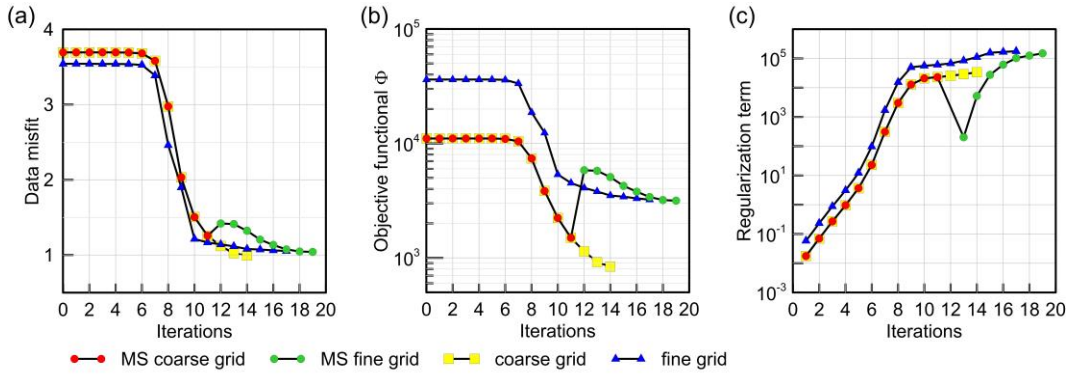

Figure 3. Inversion parameters versus iterations. (a) Data misfit (rms); (b) objective function; (c) regularization term. The red lines represent the coarse-grid inversion stage in the multiscale inversions, the green ones represent the fine-grid inversion stage in the multiscale inversion, while the yellow lines represent the inversion of coarse grid with sparse survey points, the blue lines represent the inversion of fine grid with dense survey points.

CONCLUSIONS

Based on the shearlet transform we proposed an multiscale regularized scheme from coarse to fine grids for AEM data inversions. The shearlet coefficients is updated in the sparse-domain, while the high-resolution resistivity model can be obtained in the spatial domain. By firstly reconstructing the overall structure from the inversion of sparse survey data on coarse grids and then using this integrated model as coarse-scale coefficients and adding fine-scale coefficients in the inversion of fine grids with dense survey data, we can invert the subsurface structures at high resolution. Numerical experiments with a synthetic model showed that the proposed MS inversion method can improve the computational efficiency while maintaining high resolution in AEM inversions. More complicated models will be given in our future presentations.

ACKNOWLEDGEMENTS

The paper is financially supported by the National Natural Science Foundation of China (42304149, 42030806, 42074120, 42274093, 42174167), China Postdoctoral Science Foundation (BX20220130, 2023M731265), Key National Research Project of China (2021YFB3202104).

REFERENCES

Mackie R L, Madden T R (1993). Conjugate direction relaxation solutions for 3-D magnetotelluric modeling, Geophysics, 58(7), 1052-1057.

Egbert G D, and Kelbert A (2012). Computational recipes for electromagnetic inverse problems. Geophys. J. Int., 189(1), 251-267.

Long Z, Cai H, Hu X, et al. (2020). Parallelized 3-D CSEM Inversion with Secondary Field Formulation and Hexahedral Mesh. IEEE Transactions on Geoscience and Remote Sensing, 58(10), 6812-6822.

Su Y, Yin C, Liu Y, et al. (2022). Sparse-Promoting 3-D Airborne Electromagnetic Inversion Based on Shearlet Transform. IEEE Transactions on Geoscience and Remote Sensing, 60, 1-13.

Kutyniok G, Lemvig J. and Lim W-Q (2011). Shearlets and Optimally Sparse Approximations. Shearlets: Multiscale Analysis for Multivariate Data, Birkhäuser Boston.

Farquharson C G (2008). Constructing piecewise-constant models in multidimensional minimum-structure inversions. Geophysics, 73(1), K1-K9.